Journal of Advances and Scholarly Researches in Allied Education
Vol. 12, Issue No. 2, January-2017, ISSN 2230-7540

Control of H-Dimer Development of Acridine Orange Utilizing Nano Clay Platelets

Priya[1]* Dr. Anil Kumar[2]

[1] Research Scholar of OPJS University, Churu Rajasthan

[2] Associate Professor, OPJS University, Churu Rajasthan

Abstract – The excitation vitality relocation of acridine orange (AO) immobilized in deoxyribonucleic corrosive (DNA) thin film was explored by time-settled fluorescence and fluorescence anisotropy rot estimations. Polyvinylalcohol (PVA) was utilized as a source of perspective framework. The retention and fluorescence spectra demonstrated that the atomic total was discouraged in DNA thin films instead of in PVA thin films. Time-settled fluorescence spectra of AO in DNA films proposed effcient vitality exchange from monomer to trap locales, dimers, or totals. Fluorescence lifetime of AO in DNA films was diminished with expanding divisions of AO, which proposed productive vitality relocation between intercalated AOs. The fluorescence anisotropy estimations straightforwardly bolstered the productive vitality movement between intercalated AOs. These discoveries show that the twofold helix DNA adds to the proficient vitality relocation between intercalated colors.

Keywords: Acridine Orange, DNA, Thin Films, PVA, H-DIMER, Nano Clay.

----------X----------

INTRODUCTION

Acridine orange (AO) is a metachromic color and has a place with the acridine family. AO ingests the approaching radiation in light of its ring structure. The overabundance vitality adequately goes around the ring, being circulated between the different bonds that exist inside the ring. AO stays in cationic shape at pH underneath 10 and is totally deprotonated at pH more prominent than 10 (Biswas, et. al., 2012). The essential type of AO can infiltrate into the film of a few cells by tolerating protons, though the cationic frame cannot do as such and subsequently, stays inside the cell and causes nearby particle fixation changes (Biswas, et. al., 2012). Concentrates on the cationic conduct of acridine orange in arrangement and communication with manufactured and organic frameworks were talked about by different specialists (Maiti, et. al., 1998). These planar heterocyclic sweet-smelling mixes are utilized as fluorescence colors in sub-atomic science, natural chemistry, toxicology and supramolecular science (Siskova, et. al., 2005). Watery arrangement of AO frames dimer even at low fixation (Fujimura, et. al., 2013). Surface basicity of oxygen planes of extending clay minerals are dictated by AO (Kubinyi, et. al., 2003). AO is utilized as a test for estimating pH slopes in layer vesicles (Grofcsik, et. al., 2006). Methodical investigations on the arrangement of superstructures of a planar cationic AO atom at the mica/arrangement interface by means of in situ AFM and optical waveguide spectroscopy have been accounted for by H. Yao et. al., 2005). It was seen that the color framed H-totals at the interface. Acridine orange has been generally utilized as a stainer for the portrayal of biopolymers (Czimerova, et. al., 2008). The conglomeration highlight of AO is of high significance concerning the utilization of AO as an atomic test for intercalation in DNA (Yao, et. al., 2005, Dare-Doyen, et. al., 2003, Fleming, et. al., 2011, Tanaka, et. al., 2001, Czimerova, et. al., 2007). The collaboration of AO with anionic polyelectrolytes as models has tremendous innovative applications (Biswas, et. al., 2012) (Czimerova, et. al., 2008). In another work, two new water dissolvable gold nanoparticles (AO-TEG-Au and AO-PEG-Au NPs) were arranged and described. They were balanced out by thioalkylated oligoethylene glycols and functionalized with flouorescent acridine orange (AO) subsidiaries (Hussain, et. al., 2007). An electrochemical DNA biosensor was created dependent on a gold cathode altered with a nanocomposite film produced using an ionic fluid, ZnO nanoparticles and chitosan. A solitary stranded DNA test was immobilized on this terminal. Cheng-Yu Jin et. al. considered the Cytotoxicity of Titanium Dioxide Nanoparticles in Mouse Fibroblast Cells utilizing AO as a stainer (Huang & Liang, 2013).

Then again, clay minerals, for example, smectites are notable for their capacity to adsorb natural materials and in this manner have indicated incredible guarantee for the development of half and half natural/inorganic nanomaterials because of their

extraordinary material properties, colloidal size, layered structure and nano-scale platelets molded measurements. They have high mechanical quality and strength and give one of a kind directing, semiconducting and dielectric properties. In late time organo-clay half and half film is a critical region of research and has applications in sensors, cathode modifiers, nonlinear optical gadgets and pyroelectric materials (Dey, et. al., 2008). Smectite mud minerals show a high liking for metachromic cationic colors in light of the fact that the negative charges of the smectites are remunerated by the positive charges of cationic natural materials by cation trade response. Cation trade limit (CEC) is an imperative property of mud minerals which relies upon accessible surface region, precious stone size, pH and the kind of interchangeable cation. It is generally communicated in miniaturized scale reciprocals per gram (peq g-1). The adsorption of various types of cationic colors by the trioctahedral smectite clay laponite and its consequences for the electronic ingestion and fluorescence spectra of the clay color suspension have been examined by a few scientists (Bujdak & Komadel, 1997). Guocheng et. al. announced the evacuation of acridine orange by low charge montmorillonite swelling muds and recommended that corresponding desorption of interchangeable cations from the clays going with AO adsorption affirmed cation trade as the most overwhelming system for AO expulsion (Bujdak & Iyi, 2005). Connection between color sub-atomic accumulation and layer charge of clay minerals has been contemplated before [19]. Significance of clay has been examined in detail in part 1.

Anyway the impact of nano clay platelets on acridine orange in the confined geometry of ultra-thin film was not considered previously.

Layer-by-layer (LbL) self-assembled system is a one of a kind apparatus utilized for manufacture of mono- and multilayered ultra-thin films of natural colors onto strong substrates attributable to its cost adequacy and effortlessness in creation. The LbL multilayer is shaped by the substitute affidavit of oppositely charged polyelectrolytes to such an extent that the charge wavers among positive and negative with each layer testimony. In the ongoing occasions this strategy has been reached out to a wide assortment of fascinating charged materials, metals and semiconductor nanoparticles [20]. The LbL technique has likewise been utilized for the layering of natural parts, for example, proteins, chemicals, cell layers, infections and DNA [21-24].

In the present work point by point examinations have been done to contemplate the impact of nano clay platelets on the ghostly qualities of acridine orange (AO) in Layer-by-Layer (LbL) self-assembled film. Our outcomes demonstrated that development of H-dimer of acridine orange in oneself assembled film can be controlled by the nearness of nano clay platelets. This may have application in color lasers, which require monomeric type of color. It might be referenced in this setting self-assembled film of a subordinate of acridine orange (d-AO) created by Langmuir-Blodgett (LB) strategy indicated unmistakable H-totals [25]. The arrangement of H-total is upgraded in blended film of d-AO and stearic corrosive (SA).

EXPERIMENTAL

1. Materials

Acridine orange (AO) (Mw=301.8), immaculateness > 99%, poly (acrylic corrosive) (PAA) purity> 99% and poly (allylamine hydrochloride) (PAH), virtue >99%, were acquired from Aldrich Concoction Co. what's more, were utilized as got.

2. Arrangement and film readiness

Film arrangement procedure by Layer-by-Layer (LbL) self-collected strategy has been talked about in detail in the Trial part 3.

Electrolytic arrangement showers were readied utilizing triple refined Milli-Q water (resistivity 18.2 MQ-cm). Quartz substrates were first dunked into the anionic PAA answer for 15 minutes pursued by washing in Milli-Q water showers for 2 minutes. The slides were then plunged into anionic shower arrangement of AO for 30 minutes pursued by comparable washing in a different arrangement of water shower to result one monolayer of AO-PAA LbL film. Entire arrangement was rehashed to achieve the ideal number of AO-PAA LbL films. All the adsorption systems were completed at room temperature (250C).

The consolidation of clay laponite in the LbL film was finished with the assistance of polycationic PAH watery arrangement (0.5 mg/mL). The CEC of laponite is 0.74 meq. Fluid arrangements of AO with various CEC level of clay were readied. The quartz slide was plunged in electrolytic polycation (PAH) answer for 15 minutes pursued by same flushing in water shower for 2 minutes and afterward plunged into the anionic mud scattering which is again trailed by washing activity in water shower. The slide subsequently arranged was plunged into the cationic electrolytic arrangement of AO of various CEC level of mud. Adequate time was given for testimony and drying of the slide.

The LbL film of AO was likewise arranged in various pH arrangement. A similar technique referenced above was rehashed, yet unique pH watery arrangements were utilized rather than typical fluid arrangement (pH=6.7).

3. Characterization

UV-Vis assimilation spectra were recorded utilizing an UV-Vis spectrophotometer (Lambda-25, Perkin Elmer).

Nuclear Power Microscopy (AFM) picture of monolayer AO-mud PAH LBL film was taken in air with business AFM framework (Bruker Innova). The AFM picture exhibited here was gotten in discontinuous contact (tapping) mode. Average output region was 1x1 pm2. The Si wafer substrate was utilized for the AFM estimation.

RESULT AND DISCOURSES

1. UV-Vis retention spectroscopy

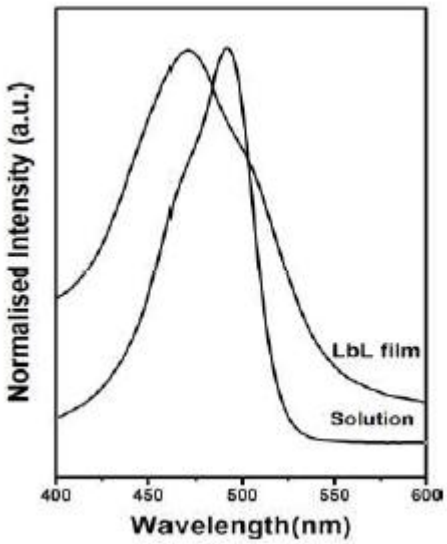

Figure 1(a). Standardized UV-Vis retention spectra of watery arrangement of AO (10'5 M) and one bi-layer LbL

The standardized UV-Vis retention spectra of watery arrangement of AO (10-5 M), and one bi-layer AO-PAA LbL film of 10-4 M AO focus are appeared in figure 1(a). AO arrangement assimilation range indicates particular and noticeable groups in the 450 nm to 540 nm locale with a solid top at 490 nm alongside a powerless shoulder at around 470 nm and is in well concurrence with the revealed outcomes [26]. The 490 nm top is because of monomer retention of AO in arrangement and the powerless shoulder at around 470 nm is because of quality of dimeric locales of AO in arrangement [26]. In the assimilation range of1 bi- layer AO-PAA LbL film, the monomer crest was decreased to a powerless protuberance and moved to 500 nm while the dimeric band ended up solid with an exceptional top at 470 nm. This dimer has been appointed as H-dimer [27]. It might be because of the way that closer relationship of AO atoms in the LbL film lead to an expansion of dimeric destinations.

Figure 1(b) demonstrates the standardized ingestion spectra for various convergence of AO in watery arrangement. It is intriguing to take note of that force of dimeric band increments with expanding arrangement focus. At higher arrangement fixation dimeric locales of AO prevail. Inset of figure 1(b) demonstrates the proportion of powers of dimeric and monomeric groups as a component of convergence of AO in arrangement. It is seen that the proportion increments bit by bit showing the power of dimeric destinations.

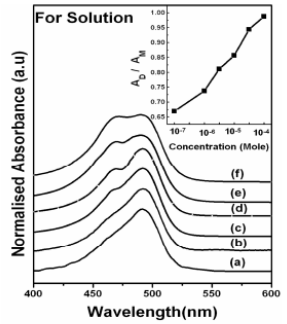

Figure 4.1(b)

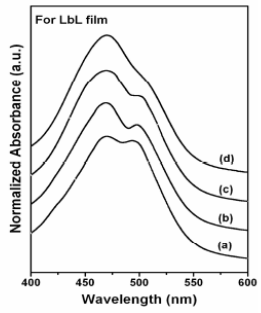

Figure 4.1(c)

Figure 1(b). Standardized ingestion spectra of AO arrangement at various fixations (a - g = 10-7 M, 10-6 M, 0.5X10-5 M, 10-5 M, 0.5X10'4 M, 10-4 M). Inset demonstrates the diagram of the proportion of dimer absorbance and monomer absorbance (Advertisement/AM) Versus convergence of AO arrangement in Mole part, (c) Standardized assimilation spectra of one bi-layer of AO-PAA LbL film at various groupings of AO (a - g = 10-7 M, 10-6 M, 10-5 M, 10-4 M).

Figure 1(c). demonstrates the standardized retention spectra of AO-PAA LbL films arranged with shifting grouping of AO. PAA being photophysically dormant, just the AO groups are watched. With expanding AO focus, dimeric band increments in power and monomeric band lessens to a frail mound. The cationic piece of AO atom cooperates with the anionic piece of the PAA particle and in this manner shapes the complex species. AO atoms draw nearer one next to the other and closer relationship of AO particles happens bringing about a great condition for total and resulting H-dimer development of AO atoms.

2. Adsorption energy

Figure 2. demonstrates the retention spectra of one bi-layer AO-PAA LbL films at various submersion times. Here in every one of the cases the inundation time in PAA was kept settled at 15 minutes, yet in the color (AO) arrangement the drenching times were changed from 5 minutes to a hour. From the figure it is seen that the power of the assimilation band increments for the films with color inundation time up to 25 minutes and remains relatively steady for the color affidavit time more prominent than 30 minutes.

This is additionally apparent from the plot of the force of the retention maxima versus time (inset of figure 2). This demonstrates the cooperation of AO atoms with the PAA layer was finished inside 30 minutes and following 30 minutes no PAA particle stayed free inside the film for further collaboration with the AO atoms.

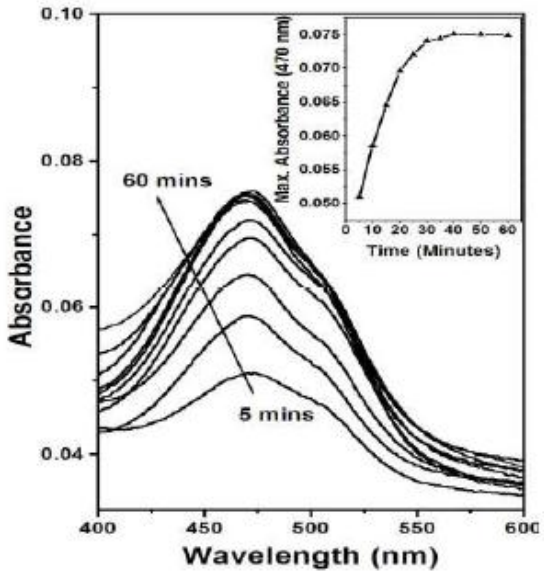

Figure 2. UV-Vis retention spectra of AO-PAA LbL films at various drenching time. Inset shows absorbance at 470 mn as an function of number of bi-layers.

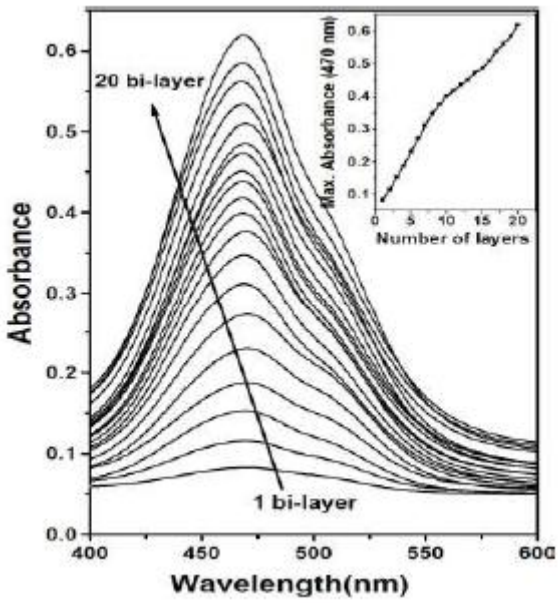

Figure 3. UV-Vis Assimilation spectra of dfferent layer AO-PAA LbL films. Inset demonstrates the plot °f the most extreme absorbance variety with time.

3. Layer Impact

UV-Vis ingestion spectra of various layered (1-20 bi-layer) AO-PAA self-assembled LbL films is appeared in figure 3. It is fascinating to take note of that retention spectra of various layered LbL films indicate relatively comparative band design independent of layer number aside from an expansion in force. This shows AO and PAA atoms are effectively moved in the LbL film amid the procedure of creation. Inset demonstrates the variety of most extreme absorbance with the layer number. It likewise bolsters the theory of effective move of atoms in the LbL film.

4. pH impact

To think about the pH impact on the LbL film, distinctive AO-PAA LbL films have been set up by utilizing watery arrangement of AO arranged at various pH esteems. Figure 4. demonstrates the ingestion spectra of one bi-layer AO-PAA LbL films stored by changing the pH of the fluid arrangement of AO (pH = 2.7, 4, 5.8, 6.6, 7.8, 8.5, 9.7, 12, 13).

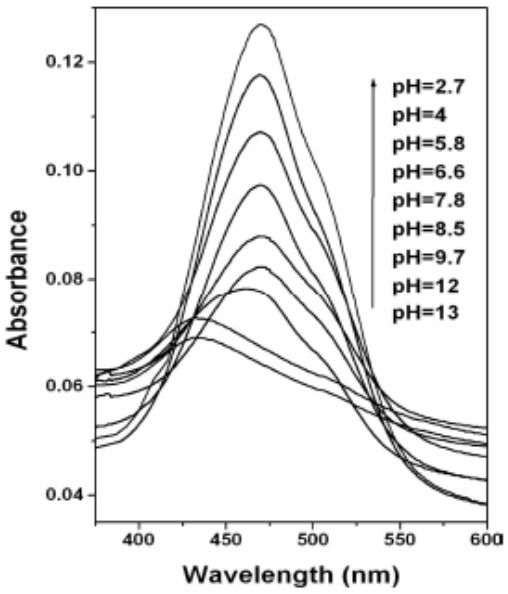

Figure 4. UV-Vis assimilation spectra of one bi-layer AO-PAA LbL film at various pH esteems

Grouping of the AO in fluid arrangement and affidavit time was kept settled at 10-4 M and 30 minutes separately for every one of the cases. At lower pH (< 10), the assimilation spectra of one bi-layer AO-PAA LbL film demonstrates the serious dimeric crest at 470 nm and the monomer top is a powerless protuberance at around 500 nm. Be that as it may, at higher pH (>10) the pinnacle is moved to shorter wavelength side. At pH 12 and 13, top emerges at around 435 nm which is blue moved regarding that at lower pH. It might be referenced in this setting comparative outcome was accounted for on the pH subordinate investigation of the retention spectra of fluid arrangement of AO (Biswas, et. al.,

2012). It was seen that at pH 12of the AO fluid arrangement (10-6-10-4 M) the retention crest appeared at 435 nm (Biswas, et. al., 2012). This is due to the essential type of AO. AO is protonated at pH bring down than 10 (pKa=10.4) due to which it can dimerize and at higher pH (>10) AO atoms get deprotonated (Biswas, et. al., 2012). From figure, it is likewise seen that the absorbance power diminishes with expanding pH esteems. This might be because of the way that at lower pH, AO particle moves toward becoming dicationic, tricationic [26], for which it can cooperate electrostatically with more anions of PAA bringing about the extraordinary retention crest. Expanding the pH esteem, AO ends up mono-cationic (protonation of ring nitrogen iota) and consequently collaborates with less number of anions of PAA which results in less power of retention top. Retention spectra of LbL film demonstrate solid likeness with the AO arrangement spectra. This demonstrates AO atoms hold its personality in the confined geometry of LbL film.

5. Effect of nano clay

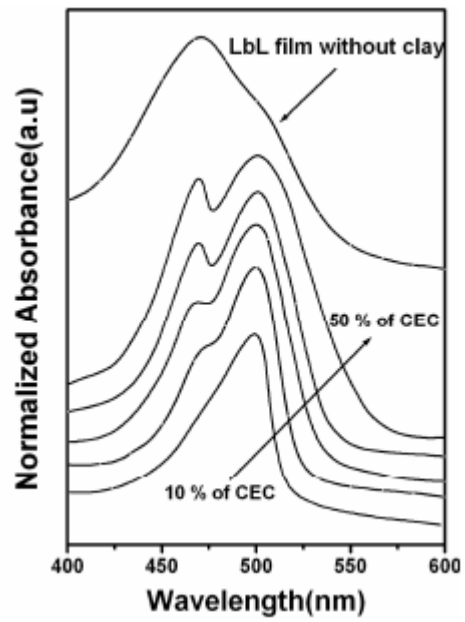

Figure 5 Standardized UV-Vis retention Spectra of AO-clay PAH one bi-layer LbL film, the stacking of AO is 10% to half of the CEC of mud laponite at 1 g/L mud in the suspension alongside the spectra of LbL film without mud.

Figure 5 demonstrates the standardized UV-Vis retention spectra of AO-clay PAH one bi-layer LbL film, the stacking of AO is 10%, 20%, 30%, 40%, half of the CEC of clay laponite at 1 g/L mud in the suspension alongside the spectra of LbL film without mud. From the figure it is seen that LbL film of AO without clay gives serious assimilation with dimeric crest at 470 nm and frail monomeric bump at 500 nm. After the incorporation of laponite nano mud platelets into the LbL film of AO, the force of monomeric crest step by step increments and the power of dimeric crest at 470 nm diminishes to a bigger degree. The power of the two groups can be controlled unequivocally by changing the stacking of AO. It might be because of the way that in the LbL film, AO atoms are adsorbed on the clay platelets by charge exchange kinds of connection. Therefore AO atoms are masterminded on the clay platelets. This decreases the likelihood of dimer development and builds monomer locales. Subsequently monomeric band increments in force.

D. Garfinkel-Shweky et.al. [28] inspected the adsorption of AO on laponite clay in watery suspension. It was seen that with expanding AO stacking into laponite clay watery suspension, at first the monomeric band diminishes with expanding of dimeric band. This was disclosed as because of flocculation of mud into watery scattering. With further increment of AO stacking, dimeric band again diminishes with further increment of monomeric band. This is because of peptization and intercalation of AO into laponite clay.

Our consequence of spectroscopic examination of the LbL film obviously shows that AO atoms are most presumably intercalated into the nano clay platelets which diminish the likelihood of dimer arrangement.

It is fascinating to make reference to in this setting so as to frame dimer, AO particles should come nearer to one another and remove between two neighboring AO atoms ought to be of the request of 0.35 nm [29] or less. Without laponite the AO atoms are adsorbed onto the foundation of PAA electrostatically onto the LbL films. In this manner AO particles come nearer to one another subsequent in an ideal condition for dimerization in LbL films.

In any case, in AO-clay PAH LbL films, at first laponite particles are joined onto the PAH spine in the films following the adsorption of cationic AO onto the laponite particles. The clay particles laponite have layer structure and have cationic trade limit [30]. In like manner the AO atoms are adsorbed onto the mud layer through cationic trade response and intercalation and therefore settled onto the mud particles in the AO-mud PAH half and half films. The adsorption of AO atoms onto the laponite particles diminishes the likelihood of dimerization in the half and half LbL films.

In one of our prior work, it has been exhibited that J-total arrangement of a thiocyanine color in Langmuir-Blodgett (LB) film can be controlled by fusing mud molecule laponite onto the LB films [31]

6. AFMstudy

The morphology and surface structure of the AO-mud PAH LbL film on Silicon wafer was contemplated by Nuclear Power Magnifying lens

(AFM). The mud particles are plainly seen in the AFM picture as appeared in figure 6(a), which affirms the development of nano dimensional organo-clay half breed LbL film. From the stature profile examination, it has been seen that the thickness of the LbL films shifts in the middle of - 2 to +2 nm. This stature incorporates the tallness of clay laponite, PAH and the AO particles onto LbL films. The AO and PAH atoms are not discernable in the AFM picture since the component of these particles are past the goals of our AFM framework.

The clay particles are thickly pressed and cover nearly the entire surface. It shows the fruitful consolidation of nano mud platelets into the cross breed organo-mud LbL film. Figure 6(b) demonstrates the harshness profile examination of AFM picture of AO-clay PAH LbL film. Harshness information was determined by the product SPIP V. 1.92. The harshness normal determined is 0.884773 nm and it is low. R.M.S. harshness is 1.2474 nm and normal stature is 4.231 nm.

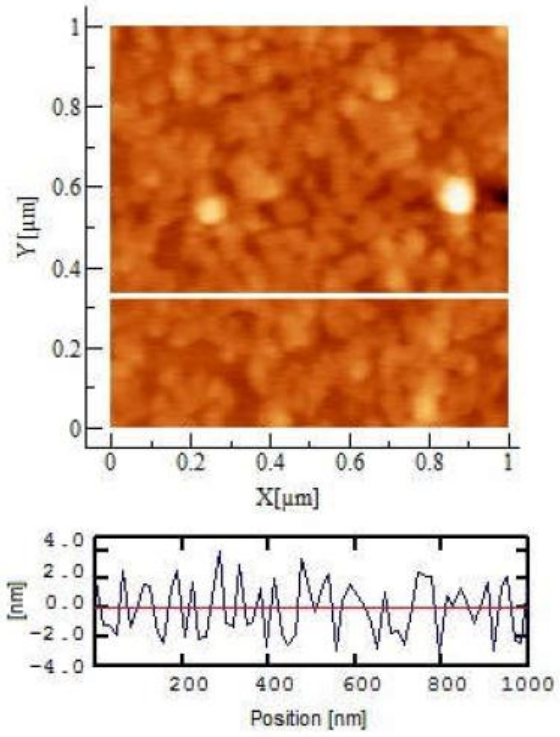

Figure 6 (a) AFM picture of AO-clay PAH LbL film on silicon wafer.

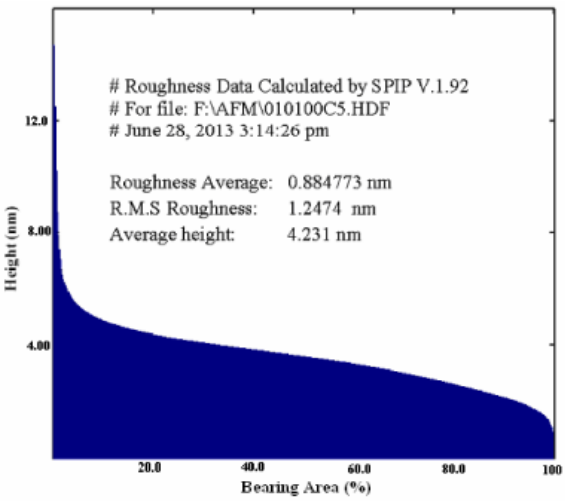

Figure 6(b). Unpleasantness profile investigation of AFM picture of AO-clay PAH LbL film.

CONCLUSION

In end our outcomes demonstrate that even in fluid arrangement of acridine orange (AO) the ingestion force of H-dimeric band increments with expanding arrangement fixation and at higher arrangement focus, dimeric band prevails. In the LbL film of AO dimeric band is profoundly extraordinary and monomeric band diminishes to a powerless mound. H-dimer development of acridine orange (AO) in oneself amassed film can be controlled by fusing nano clay platelets. This was prove from the decline of dimeric band in the UV-Vis retention spectra. AFM picture of AO-clay PAH LbL film unmistakably demonstrates the nearness of nano clay platelets in the half breed LbL films.

REFERENCES

1. S. Biswas, H-Y Ahn, M.V. Bondar (2012). K.D. Belfield, Langmuir 28, p. 1515.

2. N.C. Maiti, S. Mazumdar, N. Periasamy (1998). J. Phys. Chem. B 102, p. 1528.

3. K. Siskova, B. Vlckova, P. Mojzes (2005). J. Mol. Structure 265, p. 744.

4. T. Fujimura, T. Shimada, S. Hamatani, S. Onodera, R. Sasai, H. Inoue, S. Takagi (2013). Langmuir 29, p. 5060.

5. M. Kubinyi, A. Grofcsik, I. Papai, W.J. Jones (2003). Chem. Phys. 286, p. 81.

6. A. Grofcsik, M. Kubinyi, A. Ruzsinszky, T. Veszpremi, W.J. Jones (2000). J. Mol. Struct. 555, p. 15.

7. A. Ghanadzadeh, H. Tajalli, P. Zirack, J. Shirdel (2004). Spectrochim. Acta Part A 60, p. 2925.

8. A. Czimerova, N. Iyi, J. Bujdaka (2008). J. Colloid Interface Sci. 320, p. 140.

9. H. Yao, K. Domoto, T. Isohashi, K. Kimura (2005). Langmuir 21, p. 1067.

10. S. Dare-Doyen, D. Doizi, P. Guilbaud, F. Djedaini-Pilard, B. Perly, P. Millie (2003). J. Phys.Chem. B 107, p. 13803.

11. S. Fleming, A. Mills, T. Tuttle (2011). Beilstein J. Org. Chem. 7, p. 432.

12. K. Tanaka, T. Miura, N. Umezawa, Y. Urano, K. Kikuchi, T. Higuchi, T. Nagano (2001). J. Am. Chem. Soc. 123, p. 2530.

13. A. Czimerova, N. Iyi, J. Bujdak (2007). J. Colloid Interface Sci. 306, p. 316.

14. S.A. Hussain, P.K. Paul, D. Dey, D. Bhattacharjee, S. Sinha (2007). Chem. Phys. Lett. 450, p. 49.

15. F. Huang, H. Liang (2013). Appl. Mater. Interfaces 5, p. 5025.

16. D. Dey, M. N. Islam, S.A. Hussain, D. Bhattacharjee (2008). PRAMANA J. Phys. 71, p. 379.

17. J. Bujdak, P. Komadel (1997). J. Phys. Chem. B 101, p. 9065.

18. J. Bujdak, N. Iyi (2005). J. Phys. Chem. B 109, p. 4608.

Corresponding Author

Priya*

Research Scholar of OPJS University, Churu Rajasthan